New Journal of Physics
The open access journal at the forefront of physics

Deutsche Physikalische Gesellschaft DPG
IOP Institute of Physics

Published in partnership with: Deutsche Physikalische Gesellschaft and the Institute of Physics

OPEN ACCESS

RECEIVED
10 September 2015

REVISED
11 November 2015

ACCEPTED FOR PUBLICATION
1 December 2015

PUBLISHED
8 January 2016

PAPER

Bandwidth-resonant Floquet states in honeycomb optical lattices

A Quelle[1], **M O Goerbig**[2] **and C Morais Smith**[1]

[1] Institute for Theoretical Physics, Center for Extreme Matter and Emergent Phenomena, Utrecht University, Leuvenlaan 4, 3584 CE Utrecht, The Netherlands
[2] Laboratoire de Physique des Solides, CNRS UMR 8502, Université Paris-Sud, Bât. 510, F-91405 Orsay cedex, France

E-mail: A.Quelle@uu.nl

Keywords: Floquet, honeycomb optical lattice, topological states, quantum phase transition

Abstract

We investigate, within Floquet theory, topological phases in the out-of-equilibrium system that consists of fermions in a circularly shaken honeycomb optical lattice. We concentrate on the intermediate regime, in which the shaking frequency is of the same order of magnitude as the band width, such that adjacent Floquet bands start to overlap, creating a hierarchy of band inversions. It is shown that two-phonon resonances provide a topological phase that can be described within the Bernevig–Hughes–Zhang model of HgTe quantum wells. This allows for an understanding of out-of-equilibrium topological phases in terms of simple band inversions, similar to equilibrium systems.

1. Introduction

Ultracold atom setups provide experimentalists with a highly tunable framework that can be used to simulate quantum systems (Lewenstein *et al* 2007, Bloch *et al* 2008). For example, one can create quasi-periodic one-dimensional systems (Amico *et al* 2005), realise p-band condensates (Wirth *et al* 2011, Ölschläger *et al* 2013), or even do atomtronics (Seaman *et al* 2007), which aims at simulating electronic circuits. Due to this great flexibility, the recent realisation of topological states in condensed-matter systems (König *et al* 2007, Hasan and Kane 2010, Qi and Zhang 2010) has sparked a flurry of activities in the field of cold atoms, aiming at reproducing, engineering, and manipulating these fascinating quantum states in traps (Roncaglia *et al* 2011, Corman *et al* 2014, Burrello *et al* 2015) and in optical lattices (Hemmerich and Morais Smith 2007, Aidelsburger *et al* 2013, Miyake *et al* 2013, Jotzu *et al* 2014, Aidelsburger *et al* 2015, Chomaz *et al* 2015).

Topological fermionic systems exhibit protected conducting states at the boundary, while the bulk of the material remains insulating. In cold atoms, quantised transverse density currents play the role of the quantised charge currents, since we deal with neutral atoms in selected hyperfine states, instead of spin-full electrons. Similarly, the pair of atomic hyperfine states yields a spin-1/2 structure that allows for the analogue of quantised spin currents obtained in condensed-matter systems. The conductivity at the boundary is given by a topological invariant, which is quantised and stable against perturbations.

There are a variety of fermionic topological states known by now, and in certain cases they are well described by the ten-fold classification (Ryu *et al* 2010), which defines a topological invariant according to the symmetries and dimensionality of the system. Although well established, the ten-fold classification neglects several effects. First, it only describes systems of free fermions. Although this includes interacting systems which have a free fermionic quasiparticle description, like topological superconductors, it cannot describe strongly correlated topological phases like fractional quantum Hall systems (Tsui 1982, Laughlin 1983). It also cannot describe other interaction induced phenomena like the quantum anomalous Hall effect (Nandkishore and Levitov 2010, Jung *et al* 2011), or a quantum valley Hall effect (Marino *et al* 2015). Second, it does not consider the crystal symmetry of the lattice, which may give rise to crystalline topological insulators (TI's), and even more general behaviour (Slager *et al* 2013). Last, but not least, it does not take into account out-of-equilibrium systems.

The case of TI's under the influence of a time-periodic perturbation, the so-called Floquet TI's (FTI's) (Inoue and Tanaka 2010, Gu *et al* 2011, Kitagawa *et al* 2011, Lindner *et al* 2011, Ezawa 2013, Fregoso *et al* 2013, Rudner *et al* 2013, Wang *et al* 2013, Fregoso *et al* 2014, Gomez-Leon *et al* 2014, Perez-Piskunow *et al* 2014,

Quelle and Morais Smith 2014, Kundu *et al* 2014, Usaj *et al* 2014, Carpentier *et al* 2015), has, until now, been considered in three unequal regimes. Firstly the so-called quasi-equilibrium regime, where $J \ll \hbar\omega \ll \Delta$; here J is the hopping parameter, which is roughly the bandwidth of the relevant set of bands, ω the driving frequency, and Δ the gap between the next set of bands. In this case, the system constituents cannot follow the perturbation, and the system remains at quasi-equilibrium with simply renormalised lattice parameters. It is the regime that has been most studied (Eckardt *et al* 2005, Zenesini *et al* 2009, Koghee *et al* 2012, Struck *et al* 2013, Goldman and Dalibard 2014). Secondly, the regime where $J \ll \hbar\omega \sim \Delta$. This regime is starting to attract interest in optical lattices (Parker *et al* 2013, Zheng and Zhai 2014, Zheng *et al* 2014), but it has been unexplored in the context of condensed matter. Thirdly, the regime where $J \sim \hbar\omega \ll \Delta$, and where the equilibrium topological classification breaks down. It is this regime where most of the work on FTI's in condensed matter has taken place, and these kind of systems have even been simulated in twisted photonic waveguides (Rechtsman *et al* 2013), where the third spatial dimension takes the role of time. There have been attempts to define Chern-type topological invariants valid for every frequency range (Lindner *et al* 2011, Rudner *et al* 2013, Carpentier *et al* 2015), and it is known that these invariants reduce to the equilibrium ones in the first regime. The transition between the first and third regime has been investigated theoretically in (Kundu *et al* 2014) for graphene irradiated by circularly polarised light, and in (Gómez-León and Platero 2013) for the case of a periodically driven dimer chain. However, for the case of ultracold atoms, this regime has so far been overlooked.

Here, we show that for circularly shaken honeycomb optical lattices the transition between the first and third regime can be understood in terms of band inversion. These band inversions occur because, with decreasing frequency, the different Floquet bands start to overlap, causing a band inversion. Because the circular shaking induces phonon resonances, these band inversions cause the opening of gaps in the system that generally host topological edge states. The polarisation of the shaking breaks time-reversal symmetry, such that the resulting FTI is in class *A* of the ten-fold classification. This class also contains the quantum Hall systems, and its distinguishing feature is a quantised edge conductance, as given by the Chern number. It should be noted that this topological phase is achieved in the absence of a magnetic field, so although there are conducting edge states, no Landau levels are present in the system. It has recently been shown that one-phonon resonances create an additional topological gap in the spectrum at non-zero energy, whereas two-phonon resonances destroy the topological nature of the zero-energy gap by creating counter-propagating edge states (Quelle and Morais Smith 2014). Here, we derive an effective continuum model from the out-of-equilibrium lattice model, and show that, in the vicinity of the band inversion occurring for the two-phonon resonances, it turns out to be described by the Bernevig–Hughes–Zhang (BHZ) model (Bernevig *et al* 2006). Additionally, we demonstrate the validity of this model by comparing our results with a numerical solution of the full problem. In this way, our results describe the transition between the quasi-equilibrium and the resonant regimes of the shaken system, by modelling the appearance of phonon resonances in the latter regime in terms of band inversions. This provides a link between non-equilibrium and equilibrium topological states of matter. Finally, we discuss a possible experimental observation in shaken honeycomb optical lattices loaded with ultracold fermions, as well as in the recently realised honeycomb superlattices of CdSe nanocrystals (Boneschanscher 2014, Kalesaki *et al* 2014).

2. The Hamiltonian in co-moving coordinates

Consider an optical lattice that is shaken in time. The deviation of the lattice from its equilibrium position is denoted by $\boldsymbol{r}(t)$; by assumption $\boldsymbol{r}(t+T) = \boldsymbol{r}(t)$ for some period T. To find the Hamiltonian in co-moving coordinates, we consider the Poincaré–Cartan form

$$\mathrm{d}S = \boldsymbol{p} \cdot \mathrm{d}\boldsymbol{q} - H\mathrm{d}t \tag{1}$$

along the trajectory of a system in phase space. We change coordinates to co-moving coordinates $\tilde{\boldsymbol{q}} = \boldsymbol{q} + \boldsymbol{r}(t)$, $\tilde{\boldsymbol{p}} = \boldsymbol{p}$, such that $\mathrm{d}\tilde{\boldsymbol{p}} = \mathrm{d}\boldsymbol{p}$ and $\mathrm{d}\tilde{\boldsymbol{q}} = \mathrm{d}\boldsymbol{q} + \dot{\boldsymbol{r}}(t)\mathrm{d}t$, where $\dot{\boldsymbol{r}}(t)$ is the time derivative of $\boldsymbol{r}(t)$. The Poincaré–Cartan form can thus be rewritten as

$$\begin{aligned}\mathrm{d}S = \boldsymbol{p} \cdot \mathrm{d}\boldsymbol{q} - H\mathrm{d}t &= \tilde{\boldsymbol{p}} \cdot \left[\mathrm{d}\tilde{\boldsymbol{q}} - \dot{\boldsymbol{r}}(t)\mathrm{d}t\right] - H\mathrm{d}t \\ &= \tilde{\boldsymbol{p}} \cdot \mathrm{d}\tilde{\boldsymbol{q}} - \left(H + \tilde{\boldsymbol{p}} \cdot \dot{\boldsymbol{r}}(t)\right)\mathrm{d}t.\end{aligned} \tag{2}$$

We immediately read off the Hamiltonian in co-moving coordinates: $\tilde{H} = H + \tilde{\boldsymbol{p}} \cdot \dot{\boldsymbol{r}}(t)$. The extra term encodes the pseudoforces seen because the co-moving frame is not inertial. For a shaken optical lattice, the Hamiltonian reads

$$H = \frac{p^2}{2m} + V(\boldsymbol{q} + \boldsymbol{r}(t)), \tag{3}$$

where the potential determines the lattice, which we take to be honeycomb.

In the co-moving frame $\tilde{\boldsymbol{q}}$ and $\tilde{\boldsymbol{p}}$, equation (3) becomes

$$\begin{aligned}\tilde{H} &= \frac{\tilde{p}^2}{2m} + V\left(\tilde{\boldsymbol{q}}\right) + \tilde{\boldsymbol{p}} \cdot \dot{\boldsymbol{r}}(t) \\ &= \frac{\|\tilde{\boldsymbol{p}} + m\dot{\boldsymbol{r}}(t)\|^2}{2m} + V\left(\tilde{\boldsymbol{q}}\right) - \frac{1}{2}m\,\|\dot{\boldsymbol{r}}(t)\|^2. \end{aligned} \tag{4}$$

For circular shaking, $\boldsymbol{r}(t) = r_0(\cos(\omega t),\ \sin(\omega t))$, which means $\|\dot{\boldsymbol{r}}(t)\|^2$ is constant in time and can be ignored by shifting the energy. The circular shaking thus induces a rotating vector potential $e\boldsymbol{A}$, which has constant magnitude $eA = mr_0\omega$. This is equivalent to the Hamiltonian for a system irradiated by circularly polarised light, where $eA = eE/\omega$ for an electric field E.

3. Floquet theory

The Hamiltonian in equation (4) is periodic in time, so according to Floquet theory (Sambe 1973, Hemmerich 2010), the time-dependent Schrödinger equation has quasi-periodic solutions $\psi(t) = \exp(-i\epsilon t/\hbar)\phi(t)$, where ϕ is a periodic function in time and thus a solution of $H_F\phi(t) = \epsilon\phi(t)$. Here, the Floquet Hamiltonian is defined as $H_F := H - i\hbar\partial_t$. If H acts on the Hilbert space $\mathcal{H}$, and $\mathcal{H}_T$ is the Hilbert space of T-periodic functions, then H_F acts on $\mathcal{H} \otimes \mathcal{H}_T$. The space $\mathcal{H}_T$ is spanned by the functions $|n\rangle := \exp(in\omega t)$, and has inner product $1\int dt/T$. With respect to the states $|n\rangle$, we can write H_F as a block matrix with elements

$$\begin{aligned}\left\langle n\middle|H_F\middle|m\right\rangle &= \frac{1}{T}\int dt\, \exp\left[i\omega(m-n)t\right](H + m\hbar\omega) \\ &= H_{m-n} + m\hbar\omega\delta_{m,n}. \end{aligned} \tag{5}$$

Here, we defined H_{m-n} to be the Fourier modes of the original Hamiltonian H.

4. Model

We apply the Floquet formalism to spinless fermions in a circularly shaken honeycomb lattice, with shaking radius r_0, and frequency ω. We work in the co-moving reference frame, where the Hamiltonian has the form in equation (4). To facilitate our analysis, we use the tight-binding approximation, as done for graphene (Castro Neto *et al* 2009). In second quantisation, the result is the Bloch Hamiltonian, except that one has to account for the vector potential according to the Peierls substitution, $\boldsymbol{k} \mapsto \tilde{\boldsymbol{k}} := \boldsymbol{k} + e\boldsymbol{A}/\hbar$:

$$\tilde{H}(\boldsymbol{k},\ t) = J\sum_l \begin{pmatrix} 0 & \exp\left(i\tilde{\boldsymbol{k}}\cdot\boldsymbol{\delta}_l\right) \\ \exp\left(-i\tilde{\boldsymbol{k}}\cdot\boldsymbol{\delta}_l\right) & 0 \end{pmatrix}. \tag{6}$$

Here, $J > 0$ is the NN hopping amplitude, and our convention for the NN hopping vectors $\boldsymbol{\delta}_l$ is $\boldsymbol{\delta}_0 = a(0,\ 1)$, and $\boldsymbol{\delta}_{\pm 1} = -a(\pm\sqrt{3},\ 1)/2$, where a is the NN distance. Consequently, one obtains, via equation (5), the matrices $\tilde{H}_n$

$$\tilde{H}_n = J\begin{pmatrix} 0 & \sum_l \kappa_{-n}\exp\left[i\left(\boldsymbol{k}\cdot\boldsymbol{\delta}_l + \alpha_{l,n}\right)\right] \\ \sum_l \kappa_n \exp\left[i\left|\left(-k\cdot\boldsymbol{\delta}_l + \alpha_{l,n}\right)\right.\right] & 0 \end{pmatrix}. \tag{7}$$

In equation (7), $\kappa_n := J_n(amr_0\omega/\hbar)$, where J_n is the Bessel function of the nth kind, and $\alpha_{l,n} := n\mathrm{Arg}[\boldsymbol{\delta}_l] + n\pi/2$, where Arg gives the angle of a vector with the x-axis. Using equation (7), we obtain $\tilde{H}_F$ as an infinite block matrix

$$\tilde{H}_F = \begin{pmatrix} \ddots & \vdots & \vdots & \vdots & \vdots \\ \cdots & \tilde{H}_0 + \hbar\omega & \tilde{H}_1 & \tilde{H}_2 & \cdots \\ \cdots & \tilde{H}_{-1} & \tilde{H}_0 & \tilde{H}_1 & \cdots \\ \cdots & \tilde{H}_{-2} & \tilde{H}_{-1} & \tilde{H}_0 - \hbar\omega & \cdots \\ \vdots & \vdots & \vdots & \vdots & \ddots \end{pmatrix}. \tag{8}$$

If the spectrum around an energy $n\hbar\omega$ is desired, it can be computed by truncating the right-hand side of equation (8) around $\tilde{H}_0 + n\hbar\omega$. By tuning the shaking frequency ω, one may reach certain regimes where $\tilde{H}_F$ exhibits topological edge states. In the large-frequency limit, $\hbar\omega \gg J$, the Floquet bands are well separated, but one finds a hierarchy of band crossings upon decrease of ω, when $\hbar\omega \approx J$. These band-crossings create additional, possibly topological gaps in the spectrum. In the following, we focus on the band crossing in the

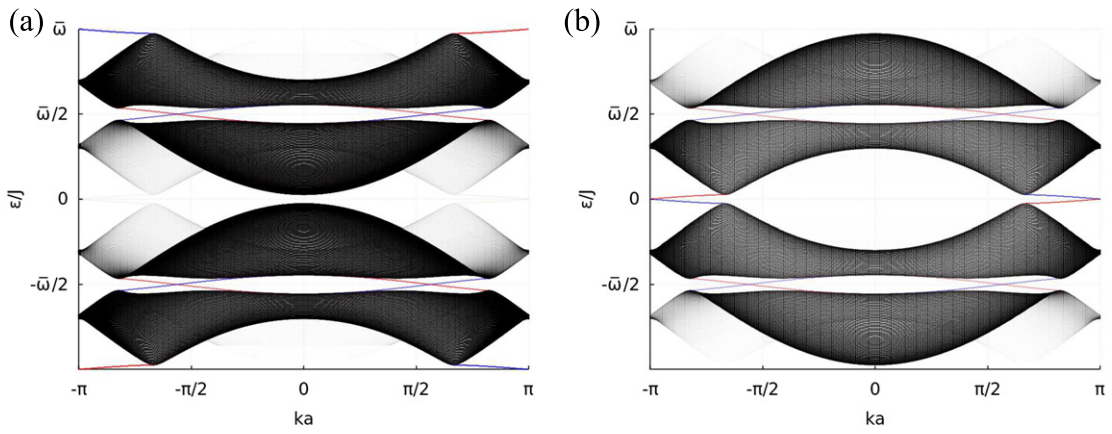

Figure 1. (a) The spectrum of the Floquet Hamiltonian $\tilde{H}_F$ is shown. Plots were made for a ribbon geometry with zigzag edges, and k denotes the Bloch momentum along the length of the ribbon. Two periods of the spectrum of $\tilde{H}_F$ are shown for $\hbar\omega = 3J$ and $m\eta_0\omega^2 a = J$. The relevant feature is the impending gap closure at $\epsilon = 0$ and $k = 0$, when the Floquet bands $n = 1$ and $n = -1$ overlap. To highlight this, we have made all bands, except for $n = 1$ and $n = -1$, translucent. Red and blue represent different edges. The y-axis is labelled in terms of $\bar{\omega} := \hbar\omega/J$. (b) The same spectrum as in (a) is shown, but now all bands except for $n = 0$ have been made translucent. This draws attention to the edge states at the Dirac points in the $\varepsilon = 0$ gap. The one-phonon resonance at $\pm\bar{\omega}/2$ is also visible in this figure, because it is caused by an overlap between the $n = 0$ and $n = \pm 1$ bands.

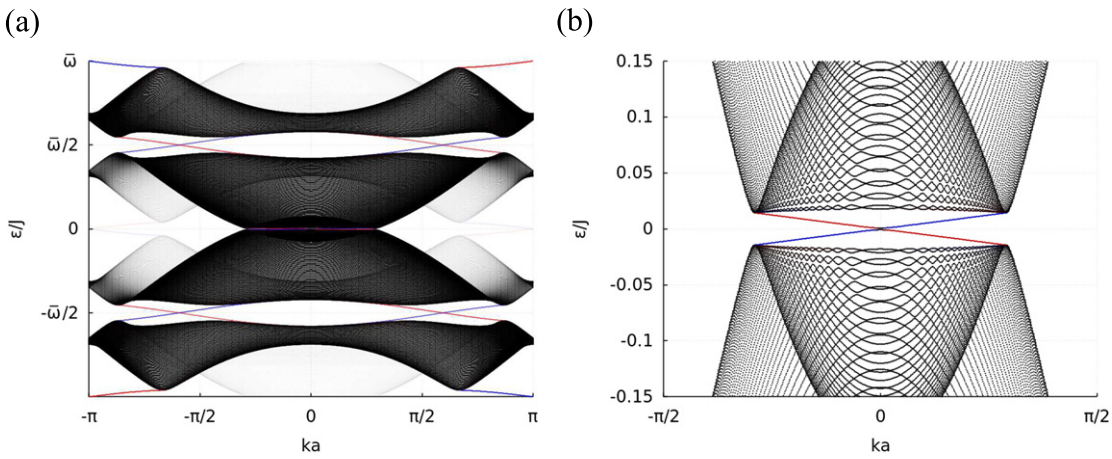

Figure 2. (a) Same as in figure 1, but for $\hbar\omega = 2.7J$. The relevant feature is the band inversion at $\epsilon = 0$ and $k = 0$, where the Floquet bands $n = 1$ and $n = -1$ overlap, creating a gap with topologically protected edge states. To highlight this, we have made all bands, except for $n = 1$ and $n = -1$, translucent. (b) A zoom in on the band crossing from (a) is provided to make the details of the gap visible.

vicinity of $k = 0$ and $\epsilon = 0$, appearing in the interesting regime: $\hbar\omega \approx 2.9J$. In figure 1, the spectrum of $\tilde{H}_F$ is plotted for $\hbar\omega = 3J$. In figure 1(a), we have made the $n = 0$ Floquet band translucent to draw attention to the impending band inversion. The bottom of the $n = 1$ valence band (on top) and the top of the $n = -1$ conduction band (below) are visible with a gap between them. In figure 1(b), the $n = 1$ and $n = -1$ Floquet bands have been made translucent to draw attention to the $n = 0$ Floquet band, which hosts topological edge states at the Dirac points. It should be noted that the bottom half of figure 1(b) is identical to the top half of figure 1(a). This is because the spectrum is periodic in $\hbar\omega$, so the $n = 0$ valence band in figure 1(b) is identical to the $n = 1$ valence band in figure 1(a). The full spectrum can be obtained by superimposing figures 1(a) and (b), since the bands $n = \pm 1$ and $n = 0$ are the only ones visible in the first two periods of the spectrum. As ω is lowered, the valence band (on top in figure 1(a)) descends and the conduction band (at the bottom of figure 1(a)) ascends; a band inversion takes place at $\hbar\omega \approx 2.9J$, and due to the radiation, the gap reopens after the bands invert (figure 2(a)). An extra pair of edge states now crosses the gap where the band inversion took place, as is highlighted in figure 2(b), where we show a zoom in on a narrow energy window. It should be noted that the edge states at the Dirac points (figure 1(b)) are still present after the band inversion, and the edge states at $k = 0$, which correspond to the two-phonon resonance, are counter-propagating with respect to them. (In figure 2, the edge states at the Dirac points have been made translucent at $\varepsilon = 0$ to avoid confusion. They are depicted at $\varepsilon = \pm\hbar\omega$, which are equivalent to $\varepsilon = 0$ due to the periodicity of the Floquet spectrum; in these gaps, instead,

the two-phonon resonance states have been made translucent.) The appearance of new edge states at $k = 0$ removes the topological protection of the edge states in the $\varepsilon = 0$ gap (Quelle and Morais Smith 2014). This can be seen by considering the topological winding number for the system (Rudner *et al* 2013). Because the two states counter-propagate, they contribute to this winding number with opposite sign, as can be checked by an explicit calculation. Furthermore, this lack of topological protection becomes evident in a lattice with armchair termination, where the zero-phonon and two-phonon resonances both occur at $k = 0$. Indeed, in this case they gap out because of hybridisation, which could not have occurred if the states were topologically protected. In contrast, if only the edge state at the Dirac points is present, changing to the armchair termination does not gap it out. Finally, it is possible to create a domain wall where the orientation of the circularly polarised light changes. This domain wall creates a boundary where the topological phase of the material changes, which causes the presence of protected states localised at the domain wall. If the counter-propagating states at $k = 0$ and the Dirac points are present, no gapless states are present at such a domain wall, which indicates that the gap must be trivial. Physically, the gapless states at the domain wall can hybridise because they can hop across the phase boundary, which causes them to gap out (Quelle *et al* 2014). These considerations show that the appearance of the two-phonon resonance indeed makes the $\varepsilon = 0$ gap trivial. The situation can be reversed by applying a staggered sublattice potential: this will destroy the zero-phonon resonance at the Dirac points, but leave the two-phonon resonance untouched. In this case, the appearance of the two-phonon resonance changes the gap at $\varepsilon = 0$ from topologically trivial to non-trivial.

5. Low-energy effective theory

To write down an effective theory that allows us to characterise the band crossing, the gap and the dispersion of the edge states, we extract the relevant energy bands from $\bar{H}_\mathrm{F}$. This is done by diagonalising $\bar{H}_0$, and for simplicity we keep terms up to second order in $\boldsymbol{k}$. We define the unitary transformation

$$U \coloneqq \frac{1}{2}\sqrt{2}\begin{pmatrix} 1 & 1 \\ 1 & -1 \end{pmatrix} \tag{9}$$

and consider the transformed Hamiltonian

$$\bar{H}_\mathrm{F} = \begin{pmatrix} \ddots & \vdots & \vdots & \vdots & \vdots \\ \cdots & \bar{H}_0 + \hbar\omega & \bar{H}_1 & \bar{H}_2 & \cdots \\ \cdots & \bar{H}_{-1} & \bar{H}_0 & \bar{H}_1 & \cdots \\ \cdots & \bar{H}_{-2} & \bar{H}_{-1} & \bar{H}_0 - \hbar\omega & \cdots \\ \vdots & \vdots & \vdots & \vdots & \ddots \end{pmatrix}, \tag{10}$$

where $\bar{H}_n = UH_nU$ by construction. From equations (7) to (9), one finds the identity

$$\bar{H}_0 = J\kappa_0\left(3 - \frac{3}{4}k^2a^2\right)\sigma_z + \ldots.$$

It follows that for $\hbar\omega \approx 3J$ and $\boldsymbol{k} \approx 0$, the $(2,\,2)$ element of the matrix $\bar{H}_0 + \hbar\omega$ and the $(1,\,1)$ element of $\bar{H}_0 - \hbar\omega$ are much smaller than all the other energy scales in the problem. They are the zeroth-order energies of the two bands near the band crossing shown in figures 1 and 2. This leads us to define a second unitary transformation V that is characterised by the matrix elements $\langle n|V|m\rangle = \sigma_+\delta_{m,n-1} + \sigma_-\delta_{m,n+1}$ and that permutes the basis vectors in such a way that the $(1,\,1)$ elements of the 2×2 matrices along the diagonal of $\bar{H}_\mathrm{F}$ are interchanged with the $(2,\,2)$ elements diagonally above. Here, $\sigma_\pm = (\sigma_x \pm \mathrm{i}\sigma_y)/2$. With respect to this basis, the Floquet Hamiltonian $\hat{H}_\mathrm{F} \coloneqq V\bar{H}_\mathrm{F}V$ reads

$$\hat{H}_\mathrm{F} = \begin{pmatrix} \ddots & \vdots & \vdots & \vdots & \vdots \\ \cdots & H_\mathrm{eff} + \hbar\omega & \hat{H}_1 & \hat{H}_2 & \cdots \\ \cdots & \hat{H}_{-1} & H_\mathrm{eff} & \hat{H}_1 & \cdots \\ \cdots & \hat{H}_{-2} & \hat{H}_{-1} & H_\mathrm{eff} - \hbar\omega & \cdots \\ \vdots & \vdots & \vdots & \vdots & \ddots \end{pmatrix}, \tag{11}$$

where the $\hat{H}_i$ are more complicated matrices obtained by interchanging elements of the $\bar{H}_j$, which do not need to be defined here. It follows that

$$H_\mathrm{eff} = \begin{pmatrix} \left(\bar{H}_0 + \hbar\omega\right)^{2,2} & \bar{H}_2^{2,1} \\ \bar{H}_{-2}^{1,2} & \left(\bar{H}_0 - \hbar\omega\right)^{1,1} \end{pmatrix}, \tag{12}$$

where the superscripts denote a specific element of the corresponding matrix. Due to its periodic structure, the matrix in equation (11) has only two eigenvalues that repeat with periodicity $\hbar\omega$. These eigenvalues correspond

to an effective 2×2 Hamiltonian that can be found through a series expansion detailed in (Goldman and Dalibard 2014). This expansion is in orders of $1/\omega$ and the size of the $\hat{H}_i$, which is $mr_0\omega$ in this specific case. The lowest order term is precisely H_{eff}, and the first correction is $[\hat{H}_{-1}, \hat{H}_1]/\omega$. All higher-order corrections have similar expressions in terms of commutators containing the $\hat{H}_i$ and powers of $1/\omega$. Because the $\hat{H}_i$ contain progressively higher orders of $mr_0\omega$, this series expansion can be truncated when the matrix elements of H_{eff} are small compared to ω, and $mr_0\omega \ll 1$. For example, $[\hat{H}_{-1}, \hat{H}_1]$ is of the same order as H_{eff}, so $[\hat{H}_{-1}, \hat{H}_1]/\omega$ is supressed by an extra factor of $1/\omega$ when the elements of H_{eff} are small. Around the two-phonon resonance, with the values of $mr_0\omega$ used to generate figures 1 and 2, all higher-order terms can be dropped from the expansion, and H_{eff} is the desired effective Hamiltonian. This can be seen from a comparison with numerical calculations, which shows that equation (12) is sufficient to accurately describe both the gap size and the presence of the topological states; see figure 2(b) for example. For small ω and/or large shaking velocities $r_0\omega$, the higher-order terms in the series do not decay, and they cannot be dropped from the expansion. The deviations caused by these extra terms have been investigated numerically in (Perez-Piskunow *et al* 2015), which describes the irradiated condensed matter analogue of this system. This system is equivalent to ours, if one sends $mr_0\omega \mapsto eE/\omega$, where E/ω is the magnitude of the vector potential describing the applied radiation. They conclude that increasing the radiation amplitude E can lead to phase transitions without additional band inversions, as the off-diagonal blocks become sizeable. This behaviour would also occur in the shaken optical lattice under an increase of $r_0\omega$ from the values used to generate figures 1 and 2.

Similarly, higher-phonon resonances occur at low values of ω and hence require the inclusion of higher-order terms in the effective Hamiltonian. Our method can also be used to model the one-phonon resonance, but the form of the effective Hamiltonian will be different, as can be seen from the different topological properties connected with this resonance. More details on the one-phonon resonance are given in the appendix. Using the definition of $\bar{H}_2$, one obtains

$$\bar{H}_2^{2,1} = \frac{3}{2}J\kappa_2\left(\mathrm{i}k_y - k_x\right) + \ldots,$$

and thus the BHZ Hamiltonian (Bernevig *et al* 2006)

$$H_{\text{eff}} = \begin{pmatrix} M + Bk^2a^2 & A\left(k_x - \mathrm{i}k_y\right)a \\ A\left(k_x + \mathrm{i}k_y\right)a & -\left(M + Bk^2a^2\right) \end{pmatrix}, \tag{13}$$

where

$$\frac{M}{J} = \frac{\hbar\omega}{J} - 3\kappa_0, \qquad \frac{B}{J} = \frac{3}{4}\kappa_0, \qquad \frac{A}{J} = -\frac{3}{2}\kappa_2. \tag{14}$$

These expressions are correct up to order $(mr_0\omega a/\hbar)^2$, and agree with the ones derived by Kundu *et al* upon replacing eE/ω by $mr_0\omega$. The presence of the Bessel function of the second kind, J_2, through κ_2 in equation (14), shows that the opening of a gap at the band inversion is a second-order phonon process. It should be noted that for the NN-hopping $J < 0$, one finds that A in equation (14) acquires an additional minus sign, but the spectrum remains unaffected. Finally, honeycomb optical lattices with a slight deformation of the unit cell that breaks the three fold symmetry at each lattice site have recently been experimentally realised (Tarruell *et al* 2012). Such an anisotropy in the unit cell will change the effective Hamiltonian since the bond length a enters it through κ_i, causing A, B, M to become direction dependent. For small anisotropies, the results discussed above should still hold, except that the precise values of $\hbar\omega$ where the two-phonon resonance occurs will depend on the renormalised A, B, M parameters, and the gap size will now become direction dependent.

6. Edge states and gap size

From the effective Hamiltonian in equation (13), and following (Qi and Zhang 2010), one can derive an explicit solution for the edge state in the infinite half-plane. Using perturbation theory to linear order in k, the edge states then disperse as

$$E_k = \pm Ak = \mp\frac{3}{16}Jka\left(\frac{mr_0\omega a}{\hbar}\right)^2 + \ldots,$$

i.e. the edge states have a velocity quadratic in the frequency ω.

From H_{eff}, an expression for the gap size Δ can also be derived, and one obtains

$$\Delta = \frac{3}{4}J\sqrt{1 - \frac{\hbar\omega}{3J}}\left(\frac{mr_0\omega a}{\hbar}\right)^2 + \ldots. \tag{15}$$

Substituting the parameter values $\hbar\omega = 2.7J$ and $mr_0\omega^2 a = J$ into equation (15) yields a gap size $\Delta = 0.033J$, which is in good agreement with the numerical results shown in figure 2(b).

7. Conclusion

In conclusion, we have investigated fermions in a circularly shaken honeycomb optical lattice in the intermediate regime, where the shaking frequency is on the order of the bandwidth $\hbar\omega \approx 3J$. In this particular regime, the system is characterised by a substantial overlap between the Floquet side bands, and a series of band inversions can be created that generally host topological edge states. We have concentrated on the crossing associated with two-phonon resonances, at $\hbar\omega \approx 2.9J$, and we have shown that the relevant effective continuum model is just the BHZ model for HgTe quantum wells. This allows for an understanding of the transition between the quasi-equilibrium regime and the resonant regime in terms of well-studied effective models, and especially in terms of band inversion, now between adjacent Floquet bands.

Considering that the model Hamiltonian also describes a honeycomb lattice irradiated with circularly polarised light, the question remains whether the discussed effects can be observed in condensed matter. In this case, the phonon resonances become photon resonances, but the prior calculations remain valid, simply by replacing $mr_0\omega$ by eE/ω. A natural candidate would be graphene, but the relevant hopping parameter $J = 2.8$ eV and the NN bond length $a = 1.4$ Å in graphene would require unphysically large frequencies beyond the THz regime, and a very high field strength of $E \approx 5.3 \cdot 10^{10}$ V m^{-1}. A more promising candidate is a self-assembled honeycomb lattice of CdSe nanocrystals (Boneschanscher 2014, Kalesaki *et al* 2014), which hosts an *s*-band exhibiting a dispersion similar to that of graphene. The hopping parameter in these artificial structures depends on the diameter and the contact area of the nanocrystals. A hopping parameter $J = 25$ meV, that is roughly two orders of magnitude smaller than that in graphene, has been theoretically predicted for nanocrystals with a diameter of 3.4 nm (Kalesaki *et al* 2014). By using light with $E = 10^7$ V m^{-1} and $\hbar\omega = 65$ meV, a gap of 1.5 meV is obtained for these parameters, which is 6% of the hopping J. In Wang *et al* (2013), the Dirac states at the surface of a 3D topological insulator are irradiated by circularly polarised light, and the resulting photon resonance gaps are detected using ARPES. Although thermal excitation of the Dirac electrons is observed, it is possible to measure the Floquet spectrum before the states have been excited away from the bands. This, together with the predicted bandgap, implies that the two-photon resonance should be observable in the recently synthesised artificial superlattices of CdSe nanocrystals (Boneschanscher 2014, Kalesaki *et al* 2014), or in predicted similar structures (Beugeling *et al* 2015).

It would be much more natural to attempt to realise the Hamiltonian in equation (13) through the use of optical lattices. Honeycomb lattices have been manufactured in the past (Soltan-Panahi *et al* 2011), and they are more promising for two reasons. The first reason for this is the much larger lattice constant, compared to condensed matter systems: since the vector potential enters the Hamiltonian in the combination eAa, this allows for smaller vector potentials. The second reason is that the circular shaking described here creates a vector potential of the form $eA = mr_0\omega$, as opposed to E/ω, so that increasing the frequency actually increases the vector potential, rather than suppressing it. In graphene, for example, the required frequencies suppress the vector potential too strongly, resulting in the necessity of unphysically large electric fields. In contrast, taking a honeycomb optical lattice with NN hopping J and recoil energy $E_r = \hbar^2k^2/2m$, we can rewrite

$$\frac{aeA}{\hbar} = \frac{ar_0\omega m}{\hbar} = \frac{1}{2}ar_0\frac{\omega\hbar}{E_r}k^2 = 2\pi^2\frac{r_0}{a}\frac{\hbar\omega}{E_r}.$$

To obtain the bandgap derived in the previous section would require shaking by a frequency $\hbar\omega = 2.7J$, at a radius $r_0 = aE_r/(140J)$. For potassium atoms loaded in an optical lattice with wavelength $k = 1064$ nm, which corresponds to $E_r \approx 4410$ Hz, the shaking would be at several kHz, with a radius of several tens of nm, which means several percent of the lattice constant. Since possible shaking amplitudes range from this regime (Jotzu *et al* 2014) up to several times the optical wavelength (Struck *et al* 2011), these parameters are easily achievable experimentally. This suggests that honeycomb optical lattices are a very promising candidate for realising the topological states discussed here. The richness of shaking protocols, which are a hallmark of optical lattices, together with these encouraging results, promise that the up-and-coming field of atomtronics could be a prime candidate for the experimental investigation of FTI's.

Acknowledgments

The authors would like to thank Daniel Vanmaekelbergh and Michelle Burrello for useful discussions. The work by A Q and C M S is part of the D-ITP consortium, a program of the Netherlands Organisation for Scientific Research (NWO) that is funded by the Dutch Ministry of Education, Culture and Science (OCW).

References

Aidelsburger M, Atala M, Lohse M, Barreiro J T, Paredes B and Bloch I 2013 *Phys. Rev. Lett.* **111** 185301
Aidelsburger M, Lohse M, Schweizer C, Atala M, Barreiro J, Nascimbnne S, Cooper N, Bloch I and Goldman N 2015 *Nat. Phys.* **11** 162
Amico L, Osterloh A and Cataliotti F 2005 *Phys. Rev. Lett.* **95** 063201
Bernevig B, Hughes T and Zhang S C 2006 *Science* **314** 1757–61
Beugeling W, Kalesaki E, Delerue C, Niquet Y M, Vanmaekelbergh D and Smith C M 2015 *Nat. Commun.* **6** 6316
Bloch I, Dalibard J and Zwerger W 2008 *Rev. Mod. Phys.* **80** 885–964
Boneschanscher M P *et al* 2014 *Science* **344** 1377–80
Burrello M, Rizzi M, Roncaglia M and Trombettoni A 2015 *Phys. Rev.* B **91** 115117
Carpentier D, Delplace P, Fruchart M and Gawedzki K 2015 *Phys. Rev. Lett.* **114** 106806
Castro Neto A, Guinea F, Peres N, Novoselov K and Geim A 2009 *Rev. Mod. Phys.* **81** 109
Chomaz L, Corman L, Bienaimé T, Desbuquois R, Weitenberg C, Nascimbène S, Beugnon J and Dalibard J 2015 *Nat. Commun.* **6** 6162
Corman L, Chomaz L, Bienaimé T, Desbuquois R, Weitenberg C, Nascimbène S, Dalibard J and Beugnon J 2014 *Phys. Rev. Lett.* **113** 135302
Eckardt A, Weiss C and Holthaus M 2005 *Phys. Rev. Lett.* **95** 260404
Ezawa M 2013 *Phys. Rev. Lett.* **110** 026603
Fregoso B M, Dahlhaus J P and Moore J E 2014 *Phys. Rev.* B **90** 155127
Fregoso B M, Wang Y H, Gedik N and Galitski V 2013 *Phys. Rev.* B **88** 155129
Goldman N and Dalibard J 2014 *Phys. Rev.* X **4** 031027
Gomez-Leon A, Delplace P and Platero G 2014 *Phys. Rev.* B **89** 205408
Gómez-León A and Platero G 2013 *Phys. Rev. Lett.* **110** 200403
Gu Z, Fertig H, Arovas D and Auerbach A 2011 *Phys. Rev. Lett.* **107** 216601
Hasan M Z and Kane C L 2010 *Rev. Mod. Phys.* **82** 3045–67
Hemmerich A 2010 *Phys. Rev.* A **81** 063626
Hemmerich A and Morais Smith C 2007 *Phys. Rev. Lett.* **99** 113002
Inoue J I and Tanaka A 2010 *Phys. Rev. Lett.* **105** 017401
Jotzu G, Messer M, Desbuquois R, Lebrat M, Uehlinger T, Greif D and Esslinger T 2014 *Nature* **515** 237
Jung J, Zhang F and MacDonald A H 2011 *Phys. Rev.* B **83** 115408
Kalesaki E, Delerue C, Morais Smith C, Beugeling W, Allan G and Vanmaekelbergh D 2014 *Phys. Rev.* X **4** 011010
Kitagawa T, Oka T, Brataas A, Fu L and Demler E 2011 *Phys. Rev.* B **84** 235108
Koghee S, Lim L K, Goerbig M and Morais Smith C 2012 *Phys. Rev.* A **85** 023637
König M, Wiedmann S, Brüne C, Roth A, Buhmann H, Molenkamp L W, Qi X L and Zhang S C 2007 *Science* **318** 766
Kundu A, Fertig H and Seradjeh B 2014 *Phys. Rev. Lett.* **113** 236803
Laughlin R B 1983 *Phys. Rev. Lett.* **50** 1395–8
Lewenstein M, Sanpera A, Ahufinger V, Damski B, Sen A and Sen U 2007 *Adv. Phys.* **56** 243–379
Lindner N, Refael G and Galitski V 2011 *Nat. Phys.* **7** 490–5
Marino E C, Nascimento L O, Alves V S and Smith C M 2015 *Phys. Rev.* X **5** 011040
Miyake H, Siviloglou G A, Kennedy C J, Burton W C and Ketterle W 2013 *Phys. Rev. Lett.* **111** 185302
Nandkishore R and Levitov L 2010 *Phys. Rev.* B **82** 115124
Ölschläger M, Kock T, Wirth G, Ewerbeck A, Smith C M and Hemmerich A 2013 *New J. Phys.* **15** 083041
Parker C V, Ha L C and Chin C 2013 *Nat. Phys.* **9** 769
Perez-Piskunow P M, Foa Torres L E F and Usaj G 2015 *Phys. Rev.* A **91** 043625
Perez-Piskunow P M, Usaj G, Balseiro C A and Torres L E F F 2014 *Phys. Rev.* B **89** 121401
Qi X L and Zhang S C 2010 *Phys. Today* **63** 33
Quelle A, Beugeling W and Morais Smith C 2014 *Solid State Commun.* **215–16** 27–33
Quelle A and Morais Smith C 2014 *Phys. Rev.* B **90** 195137
Rechtsman M, Zeuner J, Plotnik Y, Lumer Y, Podolsky D, Dreisow F, Nolte S, Segev M and Szameit A 2013 *Nature* **496** 196–200
Roncaglia M, Rizzi M and Dalibard J 2011 *Nat. Sci. Rep.* **1** 43
Rudner M, Lindner N H, Berg E and Levin M 2013 *Phys. Rev.* X **3** 031005
Ryu S, Schnyder A P, Furusaki A and Ludwig A W W 2010 *New J. Phys.* **12** 065010
Sambe H 1973 *Phys. Rev.* A **7** 2203–13
Seaman B T, Krämer M, Anderson D Z and Holland M J 2007 *Phys. Rev.* A **75** 023615
Slager R J, Mesaros A, Juričić V and Zaanen J 2013 *Nat. Phys.* **9** 98–102
Soltan-Panahi P, Struck J, Hauke P, Bick A, Plenkers W, Meineke G, Becker C, Windpassinger P, Lewenstein M and Sengstock K 2011 *Nat. Phys.* **7** 434–40
Struck J, Ölschläger C, Targat R L, Soltan-Panahi P, Eckardt A, Lewenstein M, Windpassinger P and Sengstock K 2011 *Science* **333** 996–9
Struck J *et al* 2013 *Nat. Phys.* **9** 738–43
Tarruell L, Greif D, Uehlinger T, Jotzu G and Esslinger T 2012 *Nature* **483** 302–5
Tsui D C, Stormer H L and Gossard A C 1982 *Phys. Rev. Lett.* **48** 1559–62
Usaj G, Perez-Piskunow P M, Foa Torres L E F and Balseiro C A 2014 *Phys. Rev.* B **90** 115423
Wang Y, Steinberg H, Jarillo-Herrero P and Gedik N 2013 *Science* **342** 453–7
Wirth G, Ölschläger M and Hemmerich A 2011 *Nat. Phys.* **7** 147–53
Zenesini A, Lignier H, Ciampini D, Morsch O and Arimondo E 2009 *Phys. Rev. Lett.* **102** 100403
Zheng W, Liu B, Miao J, Chin C and Zhai H 2014 *Phys. Rev. Lett.* **113** 155303
Zheng W and Zhai H 2014 *Phys. Rev.* A **89** 061603